Reducing the antenna beam pattern impact on Sentinel-1 wind fields

Dr. Sven Jacobsen, German Aerospace Center (DLR), Maritime Safety and Security Lab, Bremen, Germany
Dr. Andrey Pleskachevsky, German Aerospace Center (DLR), Maritime Safety and Security Lab, Bremen, Germany
Dr. Domenico Velotto, German Aerospace Center (DLR), Maritime Safety and Security Lab, Bremen, Germany

Abstract

A close inspection of the Sentinel-1 (S-1) Interferometric Wide Swath (IW) mode data over the ocean reveals antenna beam patterns remaining in the calibrated and noise-corrected data, resulting in discontinuous wind speed values across the beam boundaries. We present an analysis of the impact of this effect on estimated wind fields based on more than 8000 Sentinel acquisitions with level-2 OCN data available and compare to high resolution ECMWF model data. We propose a correction scheme to minimize the beam pattern impact. The method can be applied to both, level-2 OCN data products and level-1 original IW image data.

1 Introduction

The deduction of wind information over the sea surface from microwave sensor data has a long and successful history. From early scatterometer missions to the current Sentinel-1 (S-1) pair, the application of geophysical model functions (GMFs) to relate the radar backscatter to wind speed and direction in 10m height has been continuously improved. The current accuracy of SAR-based wind speeds is better than 2m/s (e.g. [1], [2], [3]) and therefore a data source appreciated by met-ocean modellers to validate and improve their models. With state of the art high resolution SAR systems wind fields with a resolution of less than 100 m are technically possible and have been successfully validated against co-located LiDAR data [4]. These data are particularly interesting for the offshore wind industry as they combine a resolution near to LiDAR capabilities and a large cross-track coverage of up to 250km for e.g. the two S-1 satellites. Such performances are obtained by implementing the TOPS SAR imaging

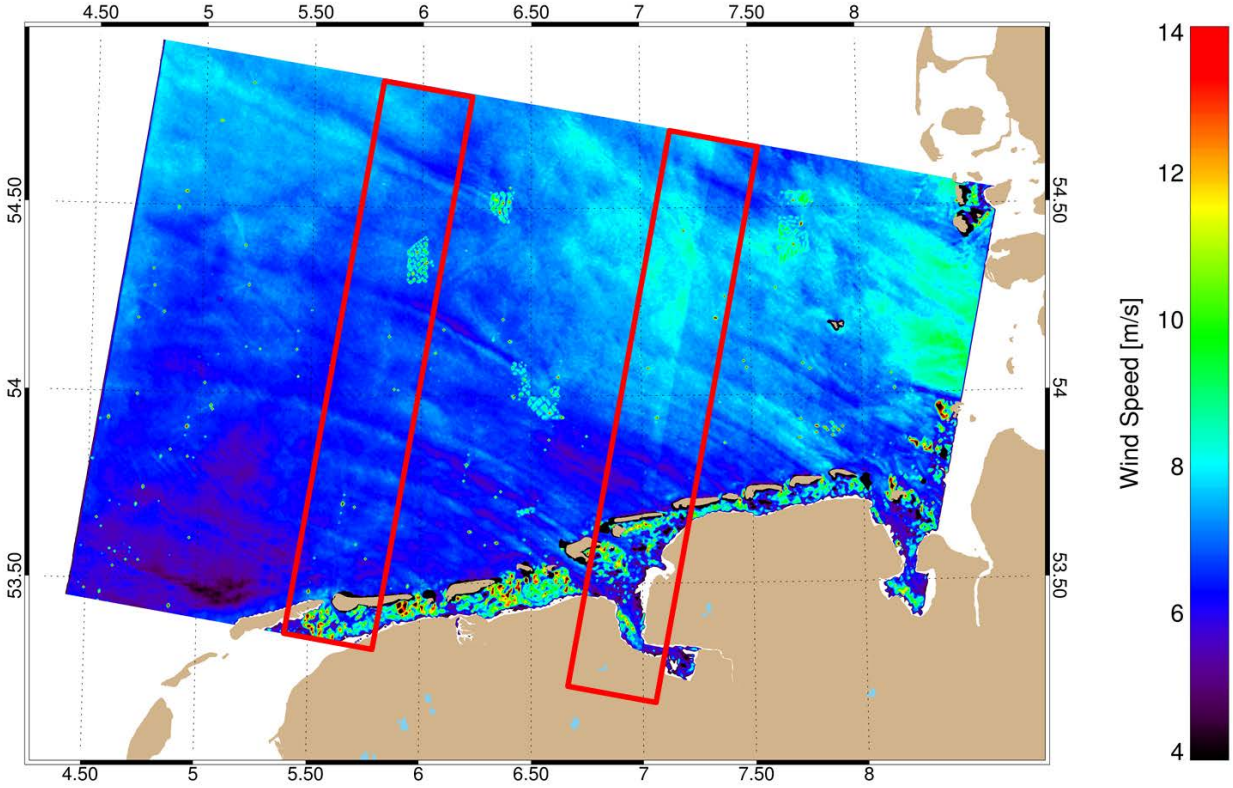

Figure 1: Wind field at 100m spatial resolution based on a Sentinel-1 IW acquisition over the German Bight from June 05, 2015. Wind from south-easterly directions creates long wind shadows behind operational wind parks. Discontinuous wind values occur across beam stitching areas marked by red boxes.

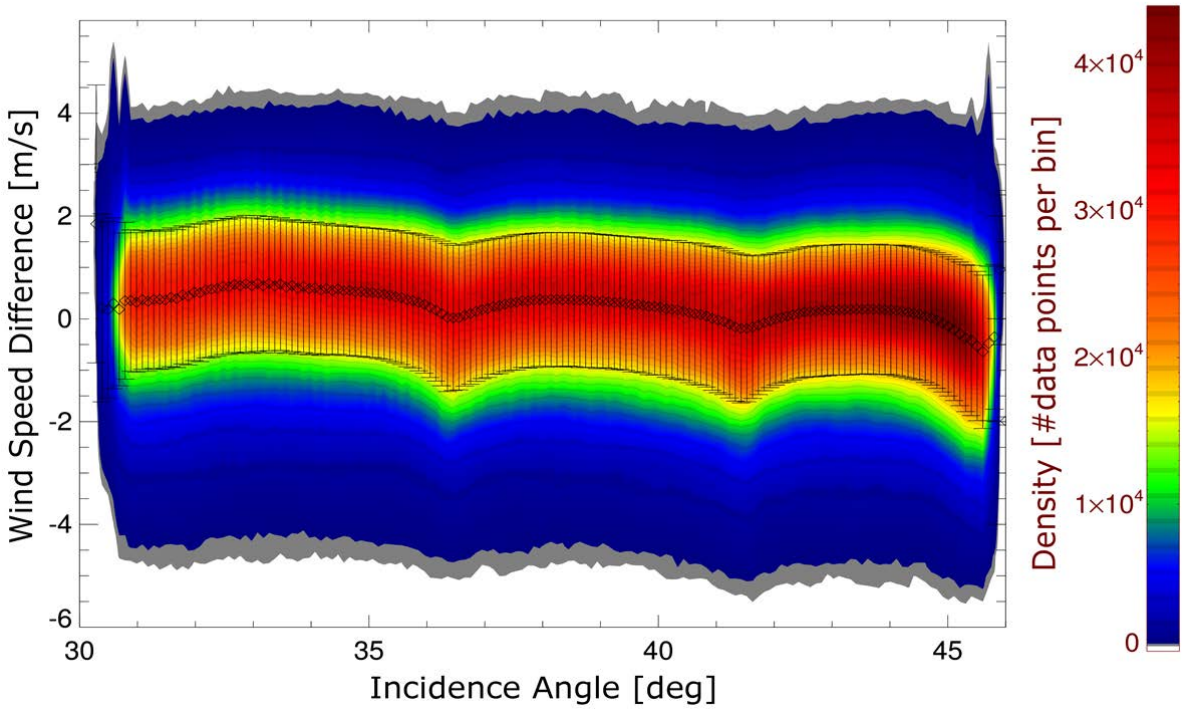

Figure 2: Histogram of the difference between ECMWF wind speed and S-1based values with respect to the incidence angle for S-1 wind values between 5 m/s and 8 m/s. Values stacked from grid values of more than 8000 OCN data products. Bin size is 0.1° times 0.1 m/s. Diamonds mark the average difference and error bars depict the standard deviation. A clear signature of the three antenna beams is visible.

mode, which has been designed to reduce the scalloping effect in burst mode SAR imaging, e.g. ScanSAR. This allows wind park operators to get regular snapshots of entire marine regions such as the German Bight and cross-validate model data especially with focus on the impact of wind shadows of adjacent turbine clusters. Figure 1 shows an example of a wind field over the German Bight from June 05, 2015. It depicts wind shadows behind operational wind parks extending up to 80km – a phenomenon that is not reliably captured by current meteorological models. This leaves large uncertainties for power production estimates for existing wind parks but more importantly for designated future wind park areas advertised for bids by the wind industry. Secondly, Figure 1 shows clear signatures of the antenna beam patterns resulting in wind speed value discontinuities across the beam stitching areas on the order of ~1m/s marked by red boxes. An error connected to these signatures is also notable in sea state fields derived from S-1 data [5].

While of minor importance when calculating coarse wind fields of several kilometres resolution, high resolution wind fields as desired by offshore wind operators suffer from this uncertainty. A compensation for these errors contained in S-1 IW wind fields would further increase the acceptance of SAR-bases wind data in both, industrial users of the data and the Numerical Weather Prediction (NWP) community for assimilation in met-ocean models.

2 Methods and Data

2.1 Data Set

Together with L1 SAR image data, the L2 Ocean (OCN) data products are provided for selected locations on the Copernicus Open Access Hub [6]. The NetCDF files contain a wind field with a resolution of ~1km by 1km and ECMWF atmospheric model data on the same grid for the acquisition time (for more information see [7]). This unique data set provides the opportunity to systematically analyse the differences between model and SAR-based wind speed values for certain incidence angles and thus revealing any correlation with antenna beam patterns. Other data streams included in the OCN data are the observed average NRCS for a grid cell and the corresponding predicted NRCS based on ECMWF wind speed and direction and using the CMOD-IFR2 GMF [7]. Hence, also differences in observed and expected NRCS can be evaluated with respect to the incidence angle. The model information is also sufficient to generate NRCS predictions and carry out the proposed analysis and comparisons with alternative GMFs. For the study presented in this paper we use all OCN data files taken over the five main acquisition areas (Gulf of Biscaya, Mediterranean, Hawaii, US East Coast and the Atlantic south of Iceland) from 10/2015 to 03/2017. The resulting data set consists of more than 8000 OCN data for IW scenes covering all kinds of wind conditions.

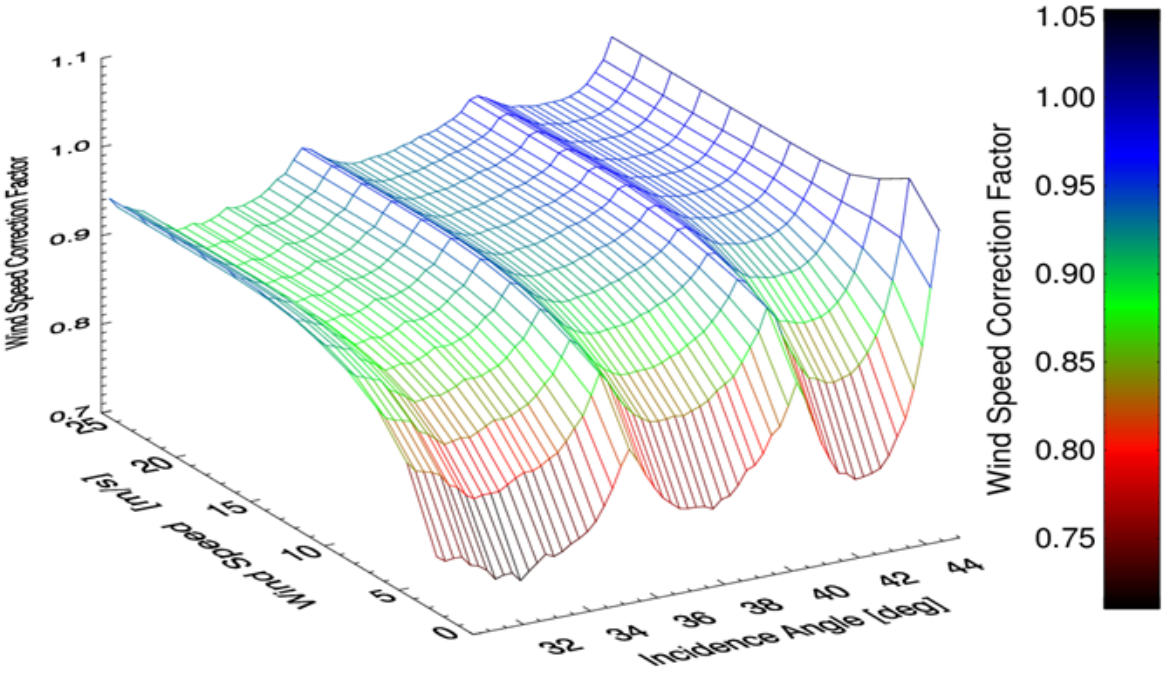

Figure 3: Correction factor field to compensate for the antenna beam impact on wind speed values. Values based on the statistical analysis as illustrated in Figure 2 and calculated for the 2D parameter field given by uncorrected S-1 wind speed regime and incidence angle.

2.2 Methods

For the first assessment of the impact of the antenna beam patterns, we subtract the ECMWF wind speed from the S1-based value for each data point and summarize the result in histogram plots with wind speed difference on the ordinate (bin size of 0.1 m/s) and the incidence angle on the abscissa (bin size of 0.1 degree). We perform this operation for different wind regimes (2-5m/s, 5-8 m/s, …, 20-23 m/s) as illustrated in Figure 2. In a second step we analyse both, the difference and the ratio between the observed NRCS and the expected value from ECMWF wind data for different regimes of NRCS in both (logarithmic and linear units).

Finally, we use the data to create correction arrays that can be applied to minimize the beam pattern impact in either OCN data products or full resolution IW images. In order to avoid inconvenient lookup tables for the operational compensation process, we approximate the arrays with a combination of functions. These correction functions are created for both, compensation of beam pattern signatures in already processed wind data and correction of the original NRCS array. Then, we analyse the agreement of ECMWF model data with the corrected data compared to the original OCN product data and quantify the improvement.

3 Results

As an exemplary excerpt from the conducted analysis Figure 2 shows the difference between S-1 and ECMWF wind speed for wind values in the range of 5-8 m/s. Characteristic patterns for the three antenna beams are clearly visible and the mean differences vary between +0.6 m/s and -0.5 m/s depending on the incidence angle under consideration. The mean values are plotted as diamond symbols and the standard deviation is marked by the error bars. The latter is in average of the order of +/- 1.5 m/s and contains a superposition of errors introduced by the accuracy of the model, the GMF used and the statistical error of the antenna beam pattern. We obtain similar curves associated with the antenna beams when analysing the NRCS difference and NRCS ratio. However, these curves differ when separately analysed for different wind speed regimes or NRSC ranges, respectively. Therefore we obtain correction factors or summands varying over the parameter space spanned by incidence angle and wind speed or mean NRCS value. Figure 3 illustrates the correction factor array for wind speeds.

The final 2D correction functions are currently applied to the entire data set and the residual differences are analysed. In the final conference paper, we will present the validated correction functions and the statistical analysis of the concerning improvement in terms of replication of ECMWF model data with the corrected OCN products. We will also present a study on the effect on wind field

discontinuities in beam stitching areas on the basis of selected level-1 S-1 IW images.

4 Discussion

While the comparison of the observed SAR wind fields to model data is not undisputed due to upsampling of the originally coarser ECMWF model data and errors or a bias within the model itself, the choice of a data set as large as used in this study minimizes these effects. The number of observations and the spread over many different regions ensures that mismatches on a single incident or regional biases average out. While a bias might still persist in the ECMWF model as such, it is believed to be negligible compared to the magnitude of the antenna beam pattern impact. Moreover the correction – regardless of whether it is applied to the NRCS values or the wind field data – always contains and compensates also the uncertainties of the GMF used. It is therefore not only a correction to minimize antenna beam pattern impact, but might also be regarded as a tweak to the GMF to improve matching with ECMWF model data. All things considered, the authors are confident that the application of the proposed correction scheme represents an improvement of the S-1 IW wind field data reliability.

5 Literature

[1] H. Hersbach, A. Stoffelen, and S. de Haan, “An improved C-band scatterometer ocean geophysical model function: CMOD5,” Journal of Geophysical Research: Oceans, vol. 112, no. C3, p. n/a–n/a, 2007.Analog Devices: Analog Design Seminar, Munich: Analog Devices GmbH, 1989

[2] X.-M. Li and S. Lehner, “Algorithm for Sea Surface Wind Retrieval From TerraSAR-X and TanDEM-X Data,” IEEE Transactions on Geoscience and Remote Sensing, vol. Early Access Online, 2013.

[3] Y. Quilfen and A. Bentamy, "Calibration/validation of ERS-1 scatterometer precision products," Geoscience and Remote Sensing Symposium, 1994. IGARSS '94. Surface and Atmospheric Remote Sensing: Technologies, Data Analysis and Interpretation., International, Pasadena, CA, USA, 1994, pp. 945-947 vol.2. doi: 10.1109/IGARSS.1994.399308

[4] S. Jacobsen, S. Lehner, J. Hieronimus, J. Schneemann, and M. Kühn, “Joint Offshore Wind Field Monitoring with Spaceborne SAR and Platform-Based Doppler Lidar Measurements”, International Archives of the Photogrammetry, Remote Sensing & Spatial Information Sciences, 2015.

[5] Pleskachevsky, A., Jacobsen, S., Tings, B. and E. Schwarz: “Sea State form Sentinel-1 Synthetic Aperture Radar Imagery for Maritime Situation Awareness” (submitted).

[6] URL: https://scihub.copernicus.eu

[7] Mouche, A. Sentinel-1 ocean wind fields (OWI) algorithm definition. In Sentinel-1 IPF Reference: (S1-TN-CLS-52-9049) Report; CLS: Brest, France, 2010; pp. 1–75.